EurJIC
European Journal of Inorganic Chemistry

Research Article
doi.org/10.1002/ejic.202300719

Chemistry Europe
European Chemical Societies Publishing

www.eurjic.org

A Family of Lanthanoid-Sodium Multifunctional Coordination Polymers: Single-Molecule Magnet, Luminescent and Magnetocaloric Properties

Alejandro Cuesta Troyano,[a] Jonay González,[a] Ana Arauzo,[b] Elena Bartolomé,[c] and E. Carolina Sañudo*[a, d]

In this paper we report the microwave assisted synthesis and characterization of a family of Na–Ln coordination polymers (CPs) of formula $[NaDy_2(MeCOO)_2(SALOH)_5(chpH)_2]$ (**1Ln**, Ln = Eu, Gd, Tb, Dy, Ho, Y). The Na^+ cations isolate Ln_2 units in a one-dimensional polymer. By changing the lanthanoid ions, we attain Single Molecule Magnet properties (**1Dy**), luminescent properties (**1Eu**, **1Tb**, **1Ho**), a diamagnetic material (**1Y**) and a material that presents magnetocaloric effect (**1Gd**).

Introduction

Lanthanoid ions are ideal candidates for the synthesis of new multifunctional materials. They combine great optical properties like emission in the visible and the near infrared (IR) along with interesting magnetic properties. Furthermore, the chemistry of lanthanoid ions is reproducible along the series of 4f Ln(III) ions, providing the possibility of creating families of complexes with tunable properties, including heterometallic complexes.

The field of single molecule magnets (SMMs) was shaken by the promise of lanthanoid-based SMMs. In the early 2000's[1–3] the first 3d–4f SMMs were reported and after that, pure 4f SMMs[4] and 3d–4f SMMs[5] have been a hot topic for synthetic coordination chemists. The inherent spin-orbit coupling in lanthanoid ions make them good candidates to prepare new SMMs with high hysteresis temperatures. In 2003 Ishikawa reported the first out-of-phase signal for lanthanoid double decker complexes, but even though the ac magnetic susceptibility data showed out-of-phase peaks at record high temperatures, this was not accompanied by the opening of hysteresis loops at similar temperatures due to quantum tunneling of the magnetization (QTM).[6–8] The opening of the hysteresis loops of the magnetization as a function of field marks the blocking temperature at which the SMM can retain its magnetization. It was not until 2017[9,10] and 2018[1,2,11] that a real breakthrough in hysteresis temperatures for lanthanoid-based SMMs was achieved. 2018, Layfield and coworkers reported an organometallic dysprociocenium complex with hysteresis loops at 80 K, above liquid nitrogen temperature. The main problem of the organometallic SMMs remains their poor stability under normal conditions. One strategy to reduce QTM and dipolar relaxation has been magnetic dilution in a diamagnetic matrix[12] or using a Lu, La or Y analogue of the compound as diamagnetic matrix.[13] In addition, dimeric Ln_2 compounds have been proposed as candidates to implement molecular quantum gates ("qugates") of qubits for Quantum Computing. These dinuclear units may be formed by two different lanthanoid ions LnLn' in distinct pocket sites,[14] or Gd_2 units with large S = 7/2 spin "qudits".[15] The organized, controlled separation of such Ln_2 units into coordination polymers represents an interesting path towards the scalability of systems. In this work, we use intrinsic magnetic dilution by introducing Na^+ ions to magnetically separate Ln_2 units in a one-dimensional coordination polymer (1D CP). We use microwave assisted synthesis to avoid lack of reproducibility and the obtention of mixtures. Microwave assisted synthesis has been used successfully by chemists[16–21] to obtain reproducible reactions and yields. Additionally, it is a clean synthesis method that can be used to further implement the Sustainable Development Goals proposed by UN (https://sdgs.un.org/), since waste production is limited and reactions are short, thus energy efficient.

Lanthanoid compounds are not only interesting for their possible SMM and qubit properties;[22] lanthanoid luminescence is a well-known property that has many interesting applications, from biomedical markers to smart anti-counterfeit inks or local thermometry.[23] Gadolinium has an isotropic half-filled shell and the highest possible S = 7/2 spin. Due to this large spin, Gd(III)

[a] A. C. Troyano, J. González, E. C. Sañudo
Secció de Química Inorgànica, Departament de Química Inorgànica i Orgànica, Facultat de Química, Universitat de Barcelona C/Martí i Franqués 1–11, 08028 Barcelona, Spain
E-mail: esanudo@ub.edu

[b] A. Arauzo
Instituto de Nanociencia y Materiales de Aragón (INMA), CSIC-Universidad de Zaragoza, and Departamento de Física de la Materia Condensada, 50009 Zaragoza, Spain

[c] E. Bartolomé
Institut de Ciència de Materials de Barcelona (ICMAB), CSIC, Campus UAB, 08193 Barcelona, Spain

[d] E. C. Sañudo
Institut de Nanociència i Nanotecnologia, IN2UB. Universitat de Barcelona C/Martí i Franqués 1–11, 08028 Barcelona, Spain

Supporting information for this article is available on the WWW under https://doi.org/10.1002/ejic.202300719

Research Article
doi.org/10.1002/ejic.202300719

complexes can display large magnetocaloric effect (MCE)[24] and are promising materials as magnetic coolants.[25,26]

One-dimensional (1D) lanthanoid-based complexes are ideal systems to investigate magnetic relaxation as a function of the type of ion (Kramer *vs.* non-Kramer), anisotropy and relative strength of intra-chain and inter-chain interactions. For example, the systematic study of the family of α-furoate-based Ln(III) coordination polymers, including $\{Ln(\alpha\text{-fur})_3\}_n$ and $\{Ln_2Ba(\alpha\text{-fur})_3\}_n$ compounds, revealed a plethora of relaxational behavior: from single-ion magnet (SIM) behavior of isolated ions in two different coordination sites in Dy compound[27] to single-chain magnet (SCM) behavior enabled by the presence of defects in antiferromagnetic (AF) Tb chains,[28] slow relaxation in Dy_2Ba[29] ferromagnetic chains transitioning to 3D order, or sluggish magnetic relaxation in Ising AF transverse Tb_2Ba chains.[30]

In this work, we report a series of isostructural $NaLn_2$ 1D coordination polymers (**1Ln**) with Ln-dependent properties that range from luminescence to SMM and MCE effect.

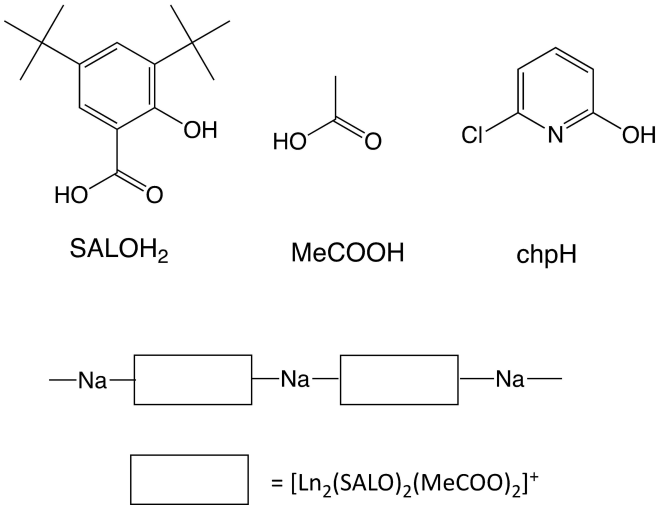

Scheme 1. Ligands used in this work (top) and schematical representation of the **1Ln** coordination polymers (bottom).

Results and Discussion

The bulkiness of 3,5-di-tert-butylsalycilic acid ($SALOH_2$), shown in Scheme 1, makes it an ideal ligand for the synthesis of lanthanoid complexes where the magnetic units must be held apart; this is crucial to reduce dipolar interactions between SMMs or qubits. Dipolar interactions that can impair SMM properties can be reduced by separating the lanthanoid centers in the crystal. Most often, this is usually done by doping the desired magnetic lanthanoid (mostly Dy and Tb) into a diamagnetic matrix of Lu, La or Y. In this work, we opt to combine two strategies: ligand bulk and a diamagnetic linker. In a previous work in heterometallic 3d–4f complexes we produced a series of SALO Mn/Ln complexes.[31] Herein, we combine a bulky ligand (SALOH, $SALOH_2$ ligand with the carboxylic acid proton removed) with a diamagnetic metal (Na^+) to attempt an intrinsically magnetically diluted system. We perform a microwave assisted reaction, using the solvent mixture of MeCN:MeOH 1:1, that has been very useful to us due to its excellent combination of a protic solvent (MeOH) and a solvent with relatively strong dipolar moment (MeCN). In this reaction we use the hydrated lanthanoid acetate salt, that has good solubility in MeCN:MeOH along with chpH (Scheme 1). ChpH can act as bridging ligand due to the terminal –OH group and it can create H-bonds that can help stabilize the obtained complexes. The microwave assisted reaction of $SALOH_2$, the lanthanoid acetate, chpH and NaOH in MeCN/MeOH 1:1 results in a colorless solution from which colorless crystals can be obtained after 10–20 days at room temperature. The crystals are identified as the series of complexes reported here: one-dimensional (1D) coordination polymers of formula $[NaLn_2(MeCOO)_2(SALOH)_5(chpH)_2]$ (**1Ln**, **Ln** = **Gd**, **Tb**, **Dy**, **Ho**, **Y**) that can be described as $[Ln_2(SALOH)_2(MeCOO)_2]^{2+}$ units linked by diamagnetic Na^+ ions and chpH, as shown in Scheme 1.

In all cases except **1Eu**, crystals suitable for single-crystal X-ray diffraction were obtained. Single crystal X-ray diffraction analyses show that all complexes are isostructural. Data collection and structural parameters are summarized in Table 1.

Table 1. Data collection and structural parameters for $[NaLn_2(MeCOO)_2(SALOH)_5(chpH)_2]$ (**1Ln**, **Ln** = **Gd**, **Tb**, **Dy**, **Ho**, **Y**).

Sample	1Gd	1Tb	1Dys	1Y	1Ho
T (K)	100	100	100	100	296
System	Monoclinic	Monoclinic	Monoclinic	Monoclinic	Monoclinic
Space group	P2(1)/m	P2(1)/m	P2(1)/m	P2(1)/m	P2(1)/m
a (Å)	9.5793(7)	9.5401(6)	9.5172(2)	9.5150(19)	9.5479(4)
b (Å)	31.727(2)	31.678(2)	31.6639(7)	31.693(6)	31.9357(13)
c (Å)	16.2410(12)	16.3157(12)	16.3315(4)	16.346(3)	16.3980(7)
alfa (°)	90	90	90	90	90
beta (°)	95.444(4)	95.526(4)	95.4930(10)	95.70(3)	96.531(3)
gamma (°)	90	90	90	90	90
V (Å^3)	4913.7(6)	4907.9(6)	4898.92(19)	4904.9(17	4967.6(4)
Gof	1.036	1.102	1.115	1.052	1.058
wR2, R1	0.1683, 0.0676	0.1614, 0.0651	0.1193, 0.0439	0.1911, 0.0704	0.1245, 0.0551
CCDC	2269645	2269641	2269642	2269644	2269643

Research Article
doi.org/10.1002/ejic.202300719

The IR of all **1Ln** complexes was practically identical, as expected for an isostructural family of complexes.

All coordination polymers crystallize in the monoclinic space group $P2_1/m$. The crystal structure of **1Dy** is shown in Figure 1. Figure S2 shows crystal structures for **1Ln**, **Ln** = **Gd**, **Tb**, **Dy**, **Ho**, **Y**. In each $[Ln_2(SALOH)_2(MeCOO)_2]^{2+}$ unit, two lanthanoid(III) ions are bonded by two SALOH ligands using their carboxylato group in a typical *syn,syn*-carboxylato bridging mode, and with the phenol group protonated. The Ln(III) centres are also bonded by two *syn,anti*-acetato ligands. The dinuclear lanthanoid units are linked into a 1D coordination polymer by sodium ions. Acetato, SALOH and chpH ligands serve as backbone for the 1D polymer, bridging Ln^{3+} and Na^+, as shown in Figure 1. The chpH ligands should be neutral for charge balance but bond valence sum (BVS) shows that the OH group is deprotonated, so that the chpH is in its zwitterionic form, that is, with the hydroxyl group deprotonated and the pyridine group protonated. One lanthanoid is octacoordinated in a distorted square-antiprism coordination environment (Dy1 in **1Dy**) and the other one is enneacoordinated in a distorted capped square antiprism coordination environment (Dy2 in **1Dy**). By looking at the average Dy–O distance for each dysprosium ion in **1Dy** one can get a sense of the size of the coordination pocket. One Ln position (Dy1 octacoordinated, average Dy1-O distance 2.374 Å) is smaller than the other one, (Dy2 enneacoordinated, average Dy2-O distance 2.425 Å). This could be exploited to discriminate between two lanthanoid ions with different size. It has been demonstrated that some systems can discriminate lanthanoid ions that show a radii difference larger than 0.06 Å.[14]

The 1-dimensional polymers are parallel to the *a*-axis of the unit cell and are well separated by the bulky tert-butyl groups of the SALOH ligands. The Dy–Dy distance in the $[Ln_2(SALOH)_2(MeCOO)_2]^+$ unit is 4.044 Å, a standard value for this type of lanthanoid-carboxylato complexes. The distance between two adjacent $[Ln_2(SALOH)_2(MeCOO)_2]^+$ units in the 1D polymer is 6.746 Å, and the closest Dy–Dy distance between 1D polymers is 14.626 Å between chains along the *c*-axis of the unit cell, and 17.807 Å along the *b*-axis. The closest Ln–Ln distances for **1Ln**, **Ln** = **Gd**, **Tb**, **Dy**, **Ho**, **Y** are reported in ESI Table S1, for the other 1Ln complexes, they are similar to those found in **1Dy**.

The bulky tert-butyl groups serve to separate the 1D chains in the crystal, providing long Ln–Ln distances and within the 1D coordination polymer the Na^+ ions separate the magnetic Ln_2 units. This should help reduce the through-space dipolar interactions and improve the SMM properties of the Dy_2 units in **1Dy**.

We attempted to prepare **1Eu**, but a large amount of precipitate is obtained from the reaction mixture after the microwave reactor. A microcrystalline material can be isolated after 2 weeks after filtration of the precipitate, in less than 5% yield. The crystalline material can be separated in small amount from the precipitate, this was enough for elemental analyses and fluorescence measurements, but not for PXRD. Elemental analysis of the crystalline material, manually separated from the precipitate indicates the formula

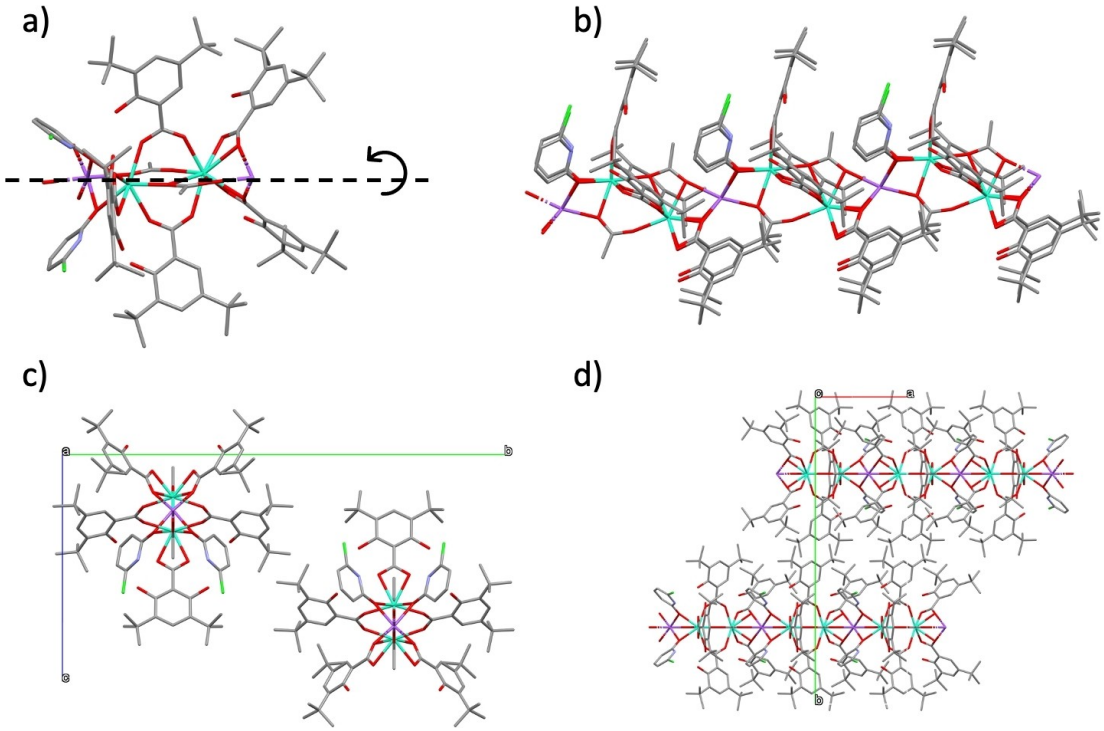

Figure 1. Crystal structure of 1D coordination polymer **1Dy**. Dy ions are shown in green and sodium ions are shown in purple. Hydrogens omitted for clarity. a) View of the $NaDy_2$ repeating unit in **1Dy** (shows two Na^+ ions for clarity). The dashed arrow is an imaginary axis along the Na^+ ions; b) shows the 1D-CP generated by growing a) on both sides and with a 90° rotation along the imaginary dashed line in Figure 1a; c) and d) show the unit cell along the *a* and *c*-axis.

Research Article
doi.org/10.1002/ejic.202300719

Chemistry Europe
European Chemical Societies Publishing

$[NaEu_2(MeCOO)_2(SALOH)_5(chpH)_2]$ for **1Eu**, with solvent molecules. However, the powder X-ray diffraction (PXRD) pattern of the precipitate was compared to the calculated PXRD pattern for the single crystals of **1Dy**, as shown in Figure S1 (ESI material). The data show that even though the same polymeric 1D structure is formed, there are also impurities in the precipitate that are mixed with the crystalline material. The family of **1Ln** compounds is a new addition to the known lanthanoid,[32–34] 3d–4f[35,36] and s block-4f[30,34] 1D coordination polymers. Usually, magnetic dilution is implemented using Y(III), La(III) or Lu(III), but Na_2Ln_4 coordination complexes containing Na+ and lanthanoid ions have also been reported.[37] For these Na_2Ln_4 complexes, the authors claim Na+ plays a structure directing role.

The magnetic properties of **1Ln**, **Ln = Gd**, **Tb**, **Dy**, **Ho** were studied in a commercial Quantum Design SQUID at applied dc fields between 0 Oe and 50 kOe. The χT vs. T data are plotted in Figure 2. The experimental χT values were 15.74 $cm^3\,K\,mol^{-1}$ for **1Gd**, 23.29 $cm^3\,K\,mol^{-1}$ for **1Tb**, 28.23 $cm^3\,K\,mol^{-1}$ for **1Dy** and 28.08 $cm^3\,K\,mol^{-1}$ for **1Ho**, in good agreement with the expected values for two non-interacting Ln(III) ions.

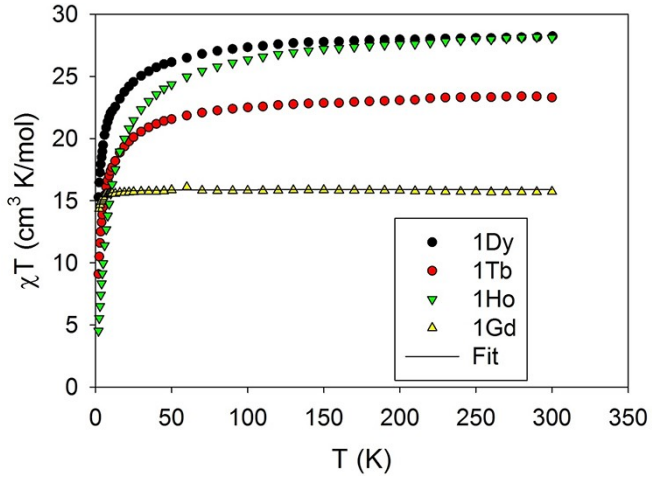

Figure 2. χT vs. T data for **1Ln**, **Ln = Gd**, **Tb**, **Dy**, **Ho** at 3000 Oe (**1Dy**, **1Gd**) and 5 kOe (**1Tb**, **1Ho**) in the 2–300 K temperature range. The solid line is the best fit to the experimental data for **1Gd** with g = 2 and J/k_B = -0.014 K.

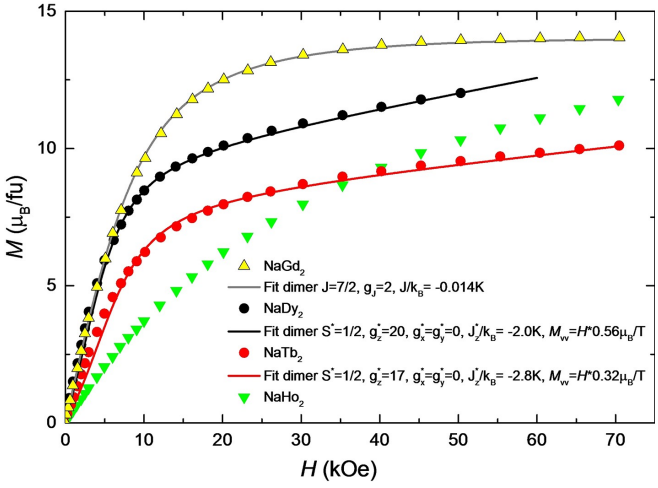

Figure 3. Magnetization as a function of the applied magnetic field for **1Ln**, **Ln = Gd**, **Tb**, **Dy**, **Ho** at 2 K, and theoretical fits within a dimer model performed with Magpack.[38]

The magnetization as a function of the applied magnetic field curves, $M(H)$, measured at 2 K for the four studied complexes are shown in Figure 3. For **1Dy** and **1Tb** coordination polymers the data could be well fit within a dimeric model of effective $S^* = 1/2$ spins, coupled antiferromagnetically (AF), and a small van Vleck contribution, with the fit parameters shown in the inset. The estimated intra-chain dimeric coupling constant amounts $J^*/k_B = -2.0$ K and $J^*/k_B = -2.8$ K for **1Dy** and **1Tb**, respectively. The data of **1Ho** could not be fit within this effective-spin model owing to the mixing with excited states, as it is also evident from the fast decay of the χT data with decreasing temperature. In the case of **1Gd**, the susceptibility $\chi T(T)$ and $M(H)$ data could be modelled with a dimer Hamiltonian shown in equation 1.

$$\mathcal{H}_{dim} = \sum_{i=1,2}\left[DS_i^{z,2} + E\left(S_i^{x,2} - S_i^{y,2}\right)\right] - 2J\left(\vec{S_1}\cdot\vec{S_2}\right) + \sum_{i=1,2} g\mu_B \vec{S_i}\cdot\vec{H} \quad (1)$$

The Hamiltonian includes terms for the zero-field splitting anisotropy, intra-dimer ion interaction and Zeeman contribution, with $g = 2.0$, negligible small D, E and J/k_B = -0.014 K. The fit is shown as a solid line in Figures 2 and 3.

Gd(III) complexes are well known to show magnetocaloric effect due to the isotropic nature of Gd(III) $4f^7$ electronic configuration. For MCE, Gd(III) ions should be isolated or very weakly coupled, thus **1Gd** is a good candidate for low temperature magnetic cooling.[24–26]

The negligible magnetic anisotropy and the small value of the exchange constant lead us to study the magnetic entropy of the system by means of magnetization vs. field curves at different temperatures. In order to investigate the possible applications of the gadolinium analog **1Gd** as a magnetic cooler, magnetization vs. field data in the 2 to 9 K temperature range were collected. Using Maxwell's equation, we calculated the magnetic entropy of **1Gd**, the data are shown in Figure 4. The maximum entropy for the system can be calculated using Boltzman's equation, that gives a value of $S_{max} = 17.64$ J/K Kg. Magnetic coupling between Gd(III) ions and crystal field anisotropy lead to smaller measured magnetic entropy change values when compared to the calculated one using Boltzman's equation. The Gd analogue **1Gd** has a magnetic entropy change of $-\Delta S_{mag} = 14.7$ J/K kg at 2 K and 70 kOe, 83% of S_{max}. The regular, widely used lanthanoid-based magnets can achieve fields of 2 T, so it is interesting to check the magnetic entropy at fields of 2 T or below. At 2 K and 2 T the value for **1Gd** is 7.9 J/K kg, 44% of the maximum entropy for **1Gd** calculated with Boltzman's equation. Two factors lead to this: on the one hand the antiferromagnetic coupling between Gd ions and the two different crystal field environments in **1Gd** lead to a reduction of the maximum possible entropy observed for **1Gd**; on the other hand, the low Gd content in **1Gd** due to the heavy SALOH ligands makes the maximum entropy of **1Gd** smaller

Research Article
doi.org/10.1002/ejic.202300719

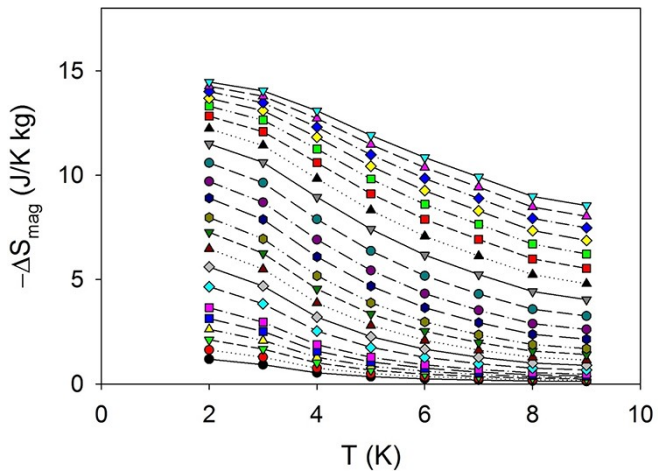

Figure 4. Magnetic entropy change plot for **1Gd** at magnetic fields between 0.5 to 0 T (black circles) and 7 to 0 T (inverted cyan triangles). The lines are only a guide for the eye.

than that of Gd metal, as usual for coordination complexes. It is often the case that high molecular weight complexes with large ligands tend to have entropies that are far from the entropy of Gd metal.

Molecular complexes show the MCE effect[39] but also coordination polymers with molecular nodes. The value obtained for the coordination polymer **1Gd** is within the values reported for similar 1D, 2D or 3D Gd(III) materials.[39–43]

There are many examples in the literature, from dinuclear complexes to 2D and 3D[44] arrays of $[Ln_2(SALOH)_2(MeCOO)_2]^+$ units or derivatives that display SMM behavior. For optimal SMM behavior, the anisotropy axes on the two Dy ions that form the unit should be parallel. The orientation of the anisotropy axes on **1Dy** can be ascertained using the software Magellan.[45] In this simple electrostatic model, the ligands are considered point charges. In **1Dy**, the axes on the two Dy ions form an angle of 86.7° (Figure 5). The dipolar interactions

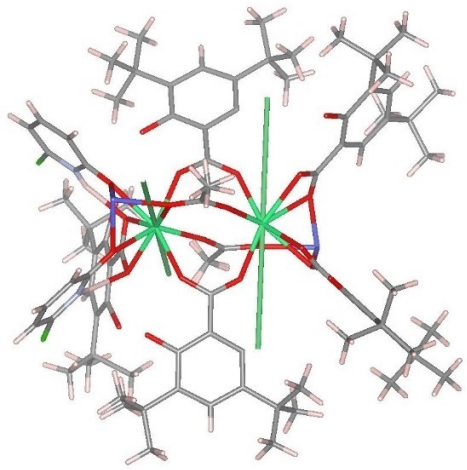

Figure 5. Anisotropy axes on the Dy ions of **1Dy**, shown as green lines, on the green Dy ions. Na ions in purple.

between the Dy ions in the dinuclear unit were calculated, within the effective Hamiltonian, with the expression:

$$J_{dip} = \frac{\mu_0}{8\pi r^3}(3\cos^2\theta_{12} - 1)\mu_B^2 g_z^{*2} \quad (2)$$

taking into account the Dy–Dy distance r and the relative orientation (θ_{12}) of the anisotropy axes calculated with Magellan. Within the dinuclear $[Dy_2(SALOH)_2(MeCOO)_2]^{2+}$ units, the dipolar coupling constant was found to be $J_{dip}/k_B = -1.896$ K. Thus, considering the intra-dimer coupling constant obtained from the fit of the $M(H)$ curve, $J/k_B = J_{dip}/k_B + J_{ex}/k_B = -2.0$ K, the exchange contribution to the interaction is estimated to be $J_{ex}/k_B = -0.104$ K.

Ac magnetic susceptibility data were collected for all complexes, but only **1Dy** showed out-of-phase AC peaks characteristic of slow relaxation of the magnetization. Figure 6 plots $\chi''(f)$ at 2 K, at different applied fields (0–50 kOe), and $\chi''(f)$ at $H = 0$ and $H = 3$ kOe at different temperatures (1.8–8 K). Two different relaxation processes are observed, one at very low frequencies (LF), ~1 Hz, and a second one at high frequencies (HF), ~7 kHz, detected in the plots at 3 kOe and 2 K. The relaxation times of both processes, τ_{LF} and τ_{HF}, as a function of the inverse of the temperature and applied magnetic field obtained from the $\chi''(f)$ plots are shown in Figure 6d and e, respectively. The LF process may be assigned to a direct process, affected by bottleneck effect. The HF process, with a temperature independent relaxation time of $\tau_{HF} \approx 2\times10^{-5}$ s, is not quenched upon the application of magnetic field. This points to a relaxation mechanism different from Quantum Tunneling of the Magnetization (QTM) of the individual Dy ions. It may be assigned to a direct process between energy levels of the dimeric Dy unit.

The holmium analogue **1Ho** displays the typical photochromic effect of Ho^{3+} salts. The crystals of **1Ho** change from yellow (incandescent lamp) to pink (fluorescent light) depending on the nature of the lamp used to generate the white light.[46] Eu and Tb analogues **1Tb** and **1Eu** were prepared to exploit the usually strong luminescence characteristic of these lanthanoid ions. Lanthanoid luminescence often relies on the antenna effect. The SALOH ligand contains a phenyl ring that could effectively act as an antenna to Tb^{3+} and Eu^{3+}, as we have shown with 2D Tb and Eu 2D MOFs.[47,48] In solution, $SALOH_2$ shows its maximum absorbance between 300 and 350 nm, depending on the solvent.[49] In order to study the luminescence of **1Tb** and **1Eu**, crushed crystals were placed in a quartz holder. For **1Eu**, a small amount of hand-picked crystals, without any precipitate were used. Using 280 nm as excitation wavelength, one can observe at room temperature the emission spectra characteristic of Tb^{3+} in **1Tb** and Eu^{3+} in **1Eu**, as shown in Figure 7. The **1Eu** emission spectra also shows a broad emission band at 430 nm that can be ascribed to the SALOH ligand (see ESI Figure S3).[49] Excitation at 330 nm produced emission spectra that saturated our detector for **1Tb**, and a lower intensity emission for **1Eu** (see ESI Figure S3), with a clear ligand centered emission at 430 nm.[49] There is thus a strong

Research Article
doi.org/10.1002/ejic.202300719

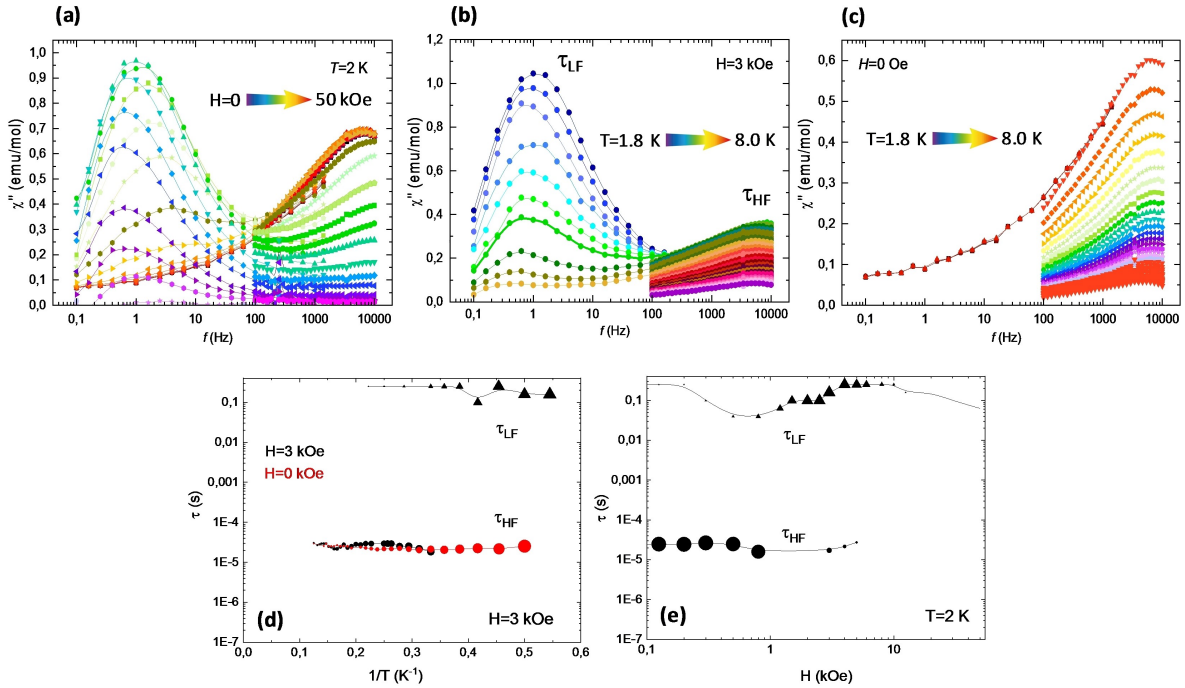

Figure 6. Top: Out-of-phase ac magnetic susceptibility data vs. frequency for **1Dy** at 2 K, (a) at applied dc fields between 0–50 kOe, (b) at 3 kOe between 1.8 K and 8.0 K, and (c) at 0 Oe and temperatures between 1.8 K and 8.0 K. Bottom: (d) relaxation time as a function of the inverse of the temperature, at $H = 0$ Oe and $H = 3$ kOe, and (e) as a function of the applied magnetic field, at $T = 2.0$ K. The relaxation times for the two observed processes are denoted τ_{LF} and τ_{HF}.

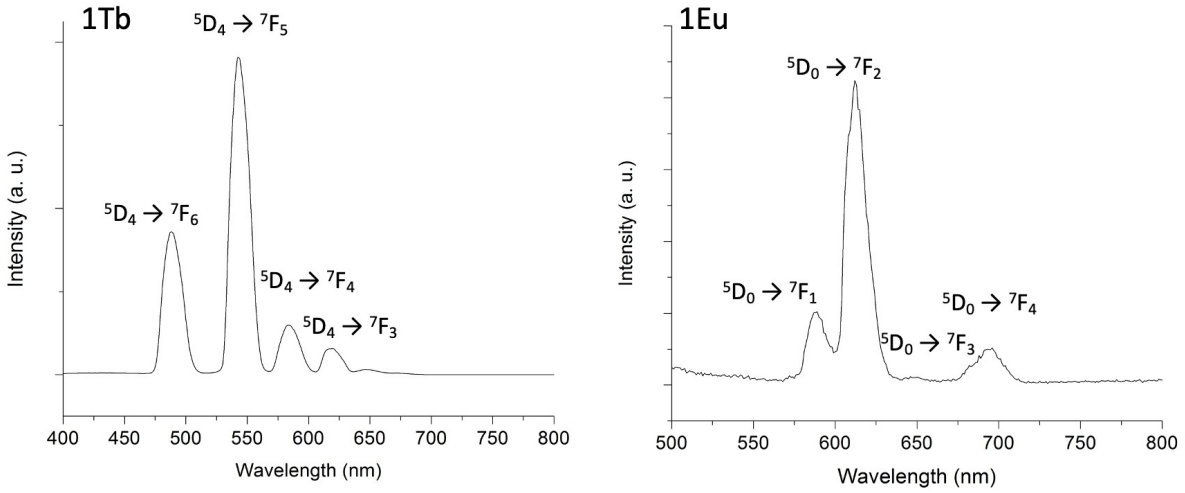

Figure 7. Emission spectra of **1Tb** and **1Eu**, with 280 nm excitation wavelength.

antenna effect for **1Tb**, but not for **1Eu**. Excitation spectra for both **1Tb** and **1Eu** are collected in ESI Figure S4.

For **1Tb**, five of the $^5D_4$ to ^7F_J (J = 6–0) transitions to the ground state multiplet of Tb(III) can be observed at 490, 545, 585, 620 and 650 nm. The main peak at 545 nm corresponds to the $^5D_4$ to $^7F_5$. The emission spectra of **1Eu** compound when exciting the phenyl group of the SALOH ligand at 280 nm shows peaks at 588, 612, 650 and 694 nm, as expected for Eu^{3+} transitions $^5D_0$ to ^7F_J (J = 0–4). The $^5D_0$ to $^7F_0$ transition is not clearly observed, this transition is only observed in C_n, C_{nv} and C_s local symmetry. Assuming the **1Eu** shares the same structure with the crystallographically characterized members of the **1Ln** family, the symmetry at the Eu center is higher since it sits on a crystallographic mirror plane. The main transitions is $^5D_0$ to $^7F_2$ centered at 612 nm, this is the electric dipole transition which is hypersensitive to the environment of the Eu(III) ion. The $^5D_0$ to $^7F_1$ is the magnetic dipole transition, with an intensity that is not affected by the coordination environment, this appears at 588 nm.[50]

Conclusions

The synthetic strategy of intrinsic magnetic dilution, that aims to isolate the magnetic units using diamagnetic linkers and bulky ligands, has been successful. The series of 1D coordination polymers **1Ln** (Ln = Eu, Gd, Dy, Tb, Ho, Y) are isolated, which form 1D chains of Ln_2 units, separated within the chain by diamagnetic Na^+ ions, and between chains by the bulky tert-butyl groups of the SALOH ligands. These dinuclear Ln_2 units, separated by the diamagnetic linkers and bulky ligands, dominate the magnetic properties of the **1Ln** series of compounds. **1Dy** shows zero-field magnetic relaxation via a fast pathway and **1Gd** displays magnetocaloric effect. Luminescent analogues can be obtained with **1Tb** and **1Eu**. As evidenced in this series, the lanthanoid ions have much to offer. A practical application of intrinsic dilution introducing diamagnetic ions like Na+ in a 1D coordination polymer of magnetic units has been demonstrated. This is a very promising synthetic strategy to exploit the desirable properties of the Ln(III) ions as SMMs, organized dinuclear qugates, or as light emitting centers. Further research efforts will be directed to exploit this idea in the obtention of 2D coordination polymers of the lanthanoid ions.

Experimental

All reagents are acquired from commercial sources and used as received.

$[NaLn_2(MeCOO)_2(SALOH)_5(chpH)_2]$ (1Ln, Ln = Eu, Gd, Tb, Dy, Ho, Y)

Sodium hydroxide (13.0 mg, 0.325 mmol), hydrated $Ln(MeCOO)_3$ (Dy = 44.1 mg, 0.13 mmol), 3,5-di-tert-butylsalycilic acid ($SALOH_2$) (81.4 mg, 0.325 mmol) and 6-chloro-2-hydroxypyridine (chpH) (16.8 mg, 0.13 mmol) were dispersed in 4 mL of 1:1 acetonitrile/methanol. The reaction mixture was placed in a microwave reactor and a pulse of 150 W was applied, with a maximum temperature of 120 °C for 10 minutes. A colorless solution was obtained that was transferred to a crystallization tube. In some cases, a white precipitate was obtained and the colorless solution was decanted and transferred to a crystallization tube. Colorless crystals grew in 10–21 days. **1Gd**, **1Tb**, **1Dy**, **1Ho** and **1Y** were characterized using single crystal X-ray diffraction. Yield of crystalline material: **1Eu** < 5%, **1Gd** 87%, **1Tb** 62% **1Dy** 75%, **1Ho** 53% and **1Y** 7%. Elemental analyses as experimental (theoretical)% for **1Eu**·$20H_2O$·2MeCN C 46.08 (46.63)%, H 4.88 (6.04)%, N 2.35 (2.34)%; **1Gd**·$6H_2O$ C 51.66 (52.62)%, H 5.80 (6.38)%, N 21.43 (1.35)%; **1Dy**·$6H_2O$·CH_3CN C 51.31 (52.27)%, H 6.26 (5.99)%, N 1.56 (1.42)%; **1Ho**·$20H_2O$ C 45.05 (45.74)%, H 5.38 (6.86)%, N 1.37 (1.19)%.

IR data (cm^{-1}, strong = s, medium = m, weak = w): 2955 (m), 2909 (w), 2870 (w), 1524 (s), 1441 (s), 1388 (s), 1362 (m), 1246 (s), 1202 (m), 1149 (w), 1127 (w), 1031 (w), 991 (w), 927 (w), 901 (w), 812 (s), 752 (w), 722 (s), 639 (w).

IR spectroscopy has been done in the University of Barcelona (UB), at the department of Inorganic and Organic Chemistry using a spectrophotometer FT-IR Nicolet iS5. PXRD was done at CCiTUB with a PANalytical X'Pert PRO MPD θ/θ powder diffractometer with Cu K_α radiation (λ = 1.5418 Å). Samples were sandwiched between films of polyester of 3.6 microns of thickness. Single crystal X-ray diffraction data for **1Gd** and **1Y** was obtained at Beamline XALOC at ALBA-Cells synchrotron. (T = 100 K, λ = 0.729 Å) The structures were solved by intrinsic phasing methods (SHELXT using the XIA package for the data collected on the beamline) and refined on F^2. Hydrogen atoms were included at the calculated positions, riding on their carrier atoms. Single crystal X-ray diffraction data for **1Dy**, **1Tb** and **1Ho** were collected on a Bruker APEXII SMART QUAZAR diffractometer using a microfocus Molybdenum kα radiation source. The structure was solved by intrinsic phasing methods (SHELXT) and refined on F^2 (SHELX). Hydrogen atoms were included on calculated positions, riding on their carrier atoms.

Photoluminescence emission and excitation spectra were measured using a spectro-fluorometer NanologTM-Horiba Jobyn Yvon at the Inorganic Chemistry section of UB. Crushed crystalline solid samples were measured between two quartz plates. Dc and ac susceptibility of powdered samples were measured, above 1.8 K, using a Quantum Design superconducting quantum interference device (SQUID) magnetometer at the Mesures Magnètiques Unit from Scientific and Technological Centers (CCiTUB), Universitat de Barcelona.

Ac measurements were done at Universidad de Zaragoza, at an excitation field of 4 Oe, at temperatures between 1.8 K–8.0 K, under dc fields between 0–30 kOe, while sweeping the frequency between 0.1 and 1000 Hz. Additional ac measurements in an extended frequency range, $10 < f < 10$ kHz, were performed in a Quantum Design PPMS ACMS susceptometer. Measurements on powdered samples were done with the addition of Daphne oil, introduced to fix the grains at low temperatures.

Acknowledgements

EB and AA acknowledge financial support from the Gobierno de Aragón (project RASMIA E12-23R). ACT, JG and ECS and EB acknowledge financial support from Spanish Ministerio de Ciencia e Innovación projects PGC2018-098630-B-I00 (ECS) and PID2022-138492NB-I00 (EB). ECS acknowledges access to XALOC ALBA-Cells beamline with project 202008445.

Conflict of Interests

The authors declare no conflict of interest.

Data Availability Statement

The data that support the findings of this study are available from the corresponding author upon reasonable request.

[1] A. Mishra, W. Wernsdorfer, K. A. Abboud, G. Christou, *J. Am. Chem. Soc.* **2004**, *126*, 15648–15649.
[2] A. Mishra, W. Wernsdorfer, S. Parsons, E. K. Brechin, *Chem. Commun.* **2005**, 2086–2088.
[3] M. Murugesu, A. Mishra, W. Wernsdorfer, K. A. Abboud, G. Christou, *Polyhedron* **2006**, *25*, 613–625.
[4] D. N. Woodruff, R. E. P. Winpenny, R. A. Layfield, *Chem. Rev.* **2013**, *113*, 5110–5148.
[5] L. Rosado Piquer, E. C. Sañudo, L. Rosado Piquer, *Dalton Trans.* **2016**, *44*, 8771–8780.
[6] N. Ishikawa, M. Sugita, T. Ishikawa, S. Y. Koshihara, Y. Kaizu, *J. Am. Chem. Soc.* **2003**, *125*, 8694–8695.

[7] N. Ishikawa, T. Iino, Y. Kaizu, *J. Phys. Chem. A* **2002**, *106*, 9543–9550.
[8] N. Ishikawa, M. Sugita, T. Ishikawa, S. Koshihara, Y. Kaizu, *J. Phys. Chem. B* **2004**, *108*, 11265–11271.
[9] F. S. Guo, B. M. Day, Y. C. Chen, M. L. Tong, A. Mansikkamäki, R. A. A. Layfield, *Angew. Chem. Int. Ed.* **2017**, *56*, 11445–11449.
[10] C. A. P. Goodwin, F. Ortu, D. Reta, N. F. Chilton, D. P. Mills, *Nature* **2017**, *548*, 439–442.
[11] F. S. Guo, B. M. Day, Y. C. Chen, M. L. Tong, A. Mansikkamäki, R. A. Layfield, *Science (1979)* **2018**, *362*, 1400–1403.
[12] F. Allouche, G. Lapadula, G. Siddiqi, W. W. Lukens, O. Maury, B. le Guennic, F. Pointillart, J. Dreiser, V. Mougel, O. Cador, C. Copéret, *ACS Cent. Sci.* **2017**, *3*, 244–249.
[13] F. Habib, P. Lin, J. Long, I. Korobkov, W. Wernsdorfer, M. Murugesu, *J. Am. Chem. Soc.* **2011**, *133*, 8830–8833.
[14] D. Aguilà, V. Velasco, L. A. Barrios, J. González-Fabra, C. Bo, S. J. Teat, O. Roubeau, G. Aromí, *Inorg. Chem.* **2018**, *57*, 8429–8439.
[15] F. Luis, P. J. Alonso, O. Roubeau, V. Velasco, D. Zueco, D. Aguilà, J. I. Martínez, L. A. Barrios, G. Aromí, *Commun. Chem.* **2020**, *3*, 1–11.
[16] B. A. Roberts, C. R. Strauss, *Acc. Chem. Res.* **2005**, *38*, 653–61.
[17] J. Klinowski, F. A. A. Paz, P. Silva, J. Rocha, *Dalton Trans.* **2011**, *40*, 321–30.
[18] C. J. Milios, A. Vinslava, A. G. Whittaker, S. Parsons, W. Wernsdorfer, G. Christou, S. P. Perlepes, E. K. Brechin, *Inorg. Chem.* **2006**, *45*, 5272–4.
[19] S. Shi, J. Hwang, *Journal of Minerals and Materials Characterization and Engineering* **2003**, *2*, 101–110.
[20] L. Rosado Piquer, E. C. Sañudo, *Polyhedron* **2019**, *169*, 195–201.
[21] L. R. Piquer, S. Dey, S. J. Teat, J. Cirera, G. Rajaraman, E. C. Sañudo, *Dalton Trans.* **2019**, *48*, 12440–12450.
[22] E. Bartolomé, A. Arauzo, J. Luzón, J. Bartolomé, F. Bartolomé, in *Handbook of Magnetic Materials*, ed. E. Brück, Elsevier, **2017**, pp. 1–289.
[23] R. Marin, G. Brunet, M. Murugesu, *Angew. Chem. Int. Ed.* **2021**, *60*, 1728–1746.
[24] M. Evangelisti, A. Candini, A. Ghirri, M. Affronte, E. K. Brechin, E. J. L. McInnes, *Appl. Phys. Lett.* **2005**, *87*, 072504.
[25] J. Romero Gómez, R. Ferreiro Garcia, A. de Miguel Catoira, M. Romero Gómez, *Renewable Sustainable Energy Rev.* **2013**, *17*, 74–82.
[26] V. K. Pecharsky, K. G. Jr. Gschneider, *J. Magn. Magn. Mater.* **1999**, *200*, 44–56.
[27] E. Bartolomé, J. Bartolomé, S. Melnic, D. Prodius, S. Shova, A. Arauzo, J. Luzón, F. Luis, C. Turta, *Dalton Trans.* **2013**, **42**, 10153–10171.
[28] E. Bartolomé, J. Bartolomé, A. Arauzo, J. Luzón, L. Badía, R. Cases, F. Luis, S. Melnic, D. Prodius, S. Shova, C. Turta, *J. Mater. Chem. C* **2016**, *4*, 5038–5050.
[29] E. Bartolomé, J. Bartolomé, S. Melnic, D. Prodius, S. Shova, A. Arauzo, J. Luzón, L. Badía-Romano, F. Luis, C. Turta, *Dalton Trans.* **2014**, *43*, 10999–11013.
[30] E. Bartolomé, A. Arauzo, J. Luzón, S. Melnic, S. Shova, D. Prodius, J. Bartolomé, A. Amann, M. Nallaiyan, S. Spagna, *Dalton Trans.* **2019**, *48*, 5022–5034.
[31] M. Ledezma-Gairaud, L. Grangel, G. Aromí, T. Fujisawa, A. Yamaguchi, A. Sumiyama, E. C. Sañudo, *Inorg. Chem.* **2014**, *53*, 5878–5880.
[32] M. Hu, H. Zhao, E. C. Sañudo, M. Chen, *Polyhedron* **2015**, *101*, 270–275, DOI: 10.1016/j.poly.2015.08.030.
[33] M. Hernández-Molina, P. A. Lorenzo-Luis, T. López, C. Ruiz-Pérez, F. Lloret, M. Julve, *CrystEngComm* **2000**, *2*, 169.
[34] E. Bartolomé, J. Bartolomé, S. Melnic, D. Prodius, S. Shova, A. Arauzo, J. Luzón, F. Luis, C. Turta, *Dalton Trans.* **2013**, *42*, 10153–10171.
[35] X. Hu, Y.-F. Zeng, Z. Chen, E. C. Sanudo, F.-C. Liu, J. Ribas, X.-He. Bu, *Cryst. Growth Des.* **2009**, *9*, 421–426.
[36] Y.-G. Huang, X.-T. Wang, F.-L. Jiang, S. Gao, M.-Y. Wu, Q. Gao, W. Wei, M.-C. Hong, *Chemistry* **2008**, **14**, 10340–7.
[37] A. Konstantatos, M. A. Sørensen, J. Bendix, H. Weihe, *Dalton Trans.* **2017**, *46*, 6024–6030.
[38] J. J. Borrás-Almenar, J. M. Clemente Juan, E. Coronado, B. S. Tsukerblat, *J. Comput. Chem.* **2001**, *22*, 985–991.
[39] S. J. Liu, S. De Han, J. P. Zhao, J. Xu, X. H. Bu, *Coord. Chem. Rev.* **2019**, *394*, 39–52.
[40] V. Zeleňák, M. Almáši, A. Zeleňáková, P. Hrubovčák, R. Tarasenko, S. Bourelly, P. Llewellyn, *Sci. Rep.* **2019**, *9*, 15572.
[41] Y. Zhu, P. Zhou, T. Li, J. Xia, S. Wu, Y. Fu, K. Sun, Q. Zhao, Z. Li, Z. Tang, Y. Xiao, Z. Chen, H.-F. Li, *Phys. Rev. B* **2020**, *102*, 144425.
[42] P. Konieczny, W. Sas, D. Czernia, A. Pacanowska, M. Fitta, R. Pełka, *Dalton Trans.* **2022**, *51*, 12762–12780.
[43] M. Kumar, L. H. Wu, M. Kariem, A. Franconetti, H. N. Sheikh, S. J. Liu, S. C. Sahoo, A. Frontera, *Inorg. Chem.* **2019**, *58*, 7760–7774.
[44] M. Chen, E. C. Sañudo, E. Jiménez, S. M. Fang, C. Sen Liu, M. Du, *Inorg. Chem.* **2014**, *53*, 6708–6714.
[45] N. F. Chilton, D. Collison, E. J. L. McInnes, R. E. P. Winpenny, A. Soncini, *Nat. Commun.* **2013**, *4*, 2551.
[46] C. H. Bellows, A. G. Clare, *Optical Materials: X* **2021**, *11*, 100077.
[47] E. Bartolomé, A. Arauzo, S. Herce, A. Palau, N. Mestres, S. Fuertes, P. Sevilla, N. S. Settineri, L. Navarro-Spreafico, J. González, E. C. Sañudo, *Molecules* **2021**, *26*, 1–14.
[48] E. Bartolomé, A. Arauzo, S. Fuertes, L. Navarro-Spreafica, P. Sevilla, H. Fernández Cortés, N. Settineri, S. J. Teat, E. C. Sañudo, *Dalton Transactions* **2023**, *52*, 7258–7270, DOI: 10.1039/D3DT00367A.
[49] K.-Y. Law, J. Shoham, *J. Phys. Chem.* **1995**, *99*, 12103–12108.
[50] K. Binnemans, *Coord. Chem. Rev.* **2015**, *295*, 1–45.

Manuscript received: November 23, 2023
Revised manuscript received: April 2, 2024
Accepted manuscript online: April 4, 2024
Version of record online: April 26, 2024